



# MiR-216a accelerates proliferation and fibrogenesis via targeting PTEN and SMAD7 in human cardiac fibroblasts

Jinsong Tao<sup>1,2#</sup>, Jingyi Wang<sup>3#</sup>, Chunyu Li<sup>4#</sup>, Weiwei Wang<sup>4</sup>, Hao Yu<sup>5</sup>, Jinhui Liu<sup>6</sup>, Xiangqing Kong<sup>1</sup>, Yan Chen<sup>5,7</sup>

<sup>1</sup>Department of Cardiology, The First Affiliated Hospital of Nanjing Medical University, Nanjing 210029, China; <sup>2</sup>Department of Cardiology, The Affiliated Hospital of Southeast University Medical College, Jiangyin 214400, China; <sup>3</sup>Department of Breast Surgery, <sup>4</sup>Intensive Care Unit, The First Affiliated Hospital of Nanjing Medical University, Nanjing 210029, China; <sup>5</sup>Emergency Center, Kizilsu Kirghiz Autonomous Prefecture People's Hospital, Artux 845350, China; <sup>6</sup>Department of Gynecology, <sup>7</sup>Emergency Center, The First Affiliated Hospital of Nanjing Medical University, Nanjing 210029, China

*Contributions:* (I) Conception and design: Y Chen; (II) Administrative support: X Kong; (III) Provision of study materials or patients: J Liu; (IV) Collection and assembly of data: H Yu, W Wang; (V) Data analysis and interpretation: C Li, J Wang; (VI) Manuscript writing: All authors; (VII) Final approval of manuscript: All authors.

<sup>#</sup>These authors contributed equally to this work.

*Correspondence to:* Dr. Xiangqing Kong. Department of Cardiology, The First Affiliated Hospital of Nanjing Medical University, 300 Guangzhou Road, Nanjing 210029, China. Email: kongxq@njmu.edu.cn; Prof. Yan Chen. Emergency Center, Kizilsu Kirghiz Autonomous Prefecture People's Hospital, Artux 845350, China. Email: yanchen\_njmu@aliyun.com.

**Background:** Heart failure (HF) is a progressive disease with relatively poor prognosis and lacks effective therapy, and the discovery of dysregulated microRNAs (miRNAs) and their role in cardiac fibroblasts have provided a new avenue for elucidating the mechanism involved in HF.

**Methods:** Two datasets of GSE53080 and GSE57338 were used to screen the miRNAs profiling and analysis the differentially expressed genes (DEGs) in HF. QRT-PCR was used to detect miR-216a between HF and healthy controls (HC). Cell counting kit-8 (CCK-8) assay and clonogenic assay were used to analyze the effect of proliferation and fibrogenesis. Then dual-luciferase activity assay and western blotting were used to confirm the key mechanism.

**Results:** In this study, the results showed that miR-216a was significantly up-regulated in HF and over-expression of miR-216a promoted proliferation and enhanced the fibrogenesis in the human cardiac fibroblasts (HCF) cells. Phosphatase and tensin homolog (PTEN) and mothers against decapentaplegic homolog 7 (SMAD7) were both validated as the direct target genes of miR-216a, which were confirmed by the dual-luciferase reporter assay. MiR-216a decreased the expression of PTEN and SMAD7 leading to the activation of Akt/mTOR and TGF- $\beta$ RI/Smad2 in the HCF cells, which might act as a promoter of cardiac fibrosis.

**Conclusions:** Our study might provide a promising approach for the treatment of HF in the future.

**Keywords:** Heart failure (HF); cardiac fibroblasts; miR-216a; phosphatase and tensin homolog (PTEN); mothers against decapentaplegic homolog 7 (SMAD7)

Submitted Sep 01, 2019. Accepted for publication Nov 04, 2019.

doi: 10.21037/cdt.2019.11.06

View this article at: <http://dx.doi.org/10.21037/cdt.2019.11.06>

## Introduction

Chronic heart failure (CHF) is a highly prevalent, progressive, multi-system disease, characterized by persistent low ventricular pump and/or filling function. Despite of numerous etiologies, ventricular remodeling is the basis for the development of CHF, including the reactive changes of cardiac myocytes and cardiac fibrosis, and the latter is the common pathology of HF caused by many etiologies (1). Cardiac fibrosis not only destroys the physiological elastic fiber skeleton of the heart, resulting in increased cardiac stiffness, which may directly contribute to both systolic and diastolic dysfunction in nearly all types of cardiac injury, but also provides potential electrophysiological matrix for cardiac death caused by malignant arrhythmias, seriously affecting the outcome of chronic HF (2,3). Cardiac fibroblasts play an important role in normal cardiac function, as well as in the fibrosis process during the CHF. Recently, studies have shown that plenty of microRNAs (miRNAs) such as miR-98, miR-19a-3p/19b-3p and miR-122 could provoke in the human cardiac fibroblasts (HCF) cells via activation of the TGF- $\beta$ 1 signaling pathways (4-6).

Exactly, miRNAs as a class of small noncoding RNAs binding incomplete complementary sequences of mRNAs, repressing translation or degrading target genes, have been found to be involved in the development of many disorders including HF (7,8). The alterations in their expression level might play crucial role in the ventricular remodeling, especially in the occurrence and progress of the cardiac fibrosis. The balancing and tight regulation of a specific miRNA might awaken the HCF cells and could be a key to drive the fibrogenesis (7,8). In this study, we showed that miR-216a was significantly up-regulated in the HF and over-expression of miR-216a promoted proliferation and enhanced the fibrogenesis in the HCF cells. Moreover, phosphatase and tensin homolog (PTEN) and mothers against decapentaplegic homolog 7 (SMAD7) were both the direct target genes of miR-216a, which were inhibited by miR-216a leading to the activation of Akt/mTOR and TGF- $\beta$ RI/Smad2 in the HCF cells. Finally, we demonstrated here that miR-216a might regulate cardiac fibrosis, at least partially, via targeting the PTEN and SMAD7 in the HCF cells.

## Methods

### *Participants and samples*

Approval for this study was obtained from the medical ethics committee of the First Affiliated Hospital of Nanjing Medical University (The number of ethics is 2015-SRFA-085). Sixty-four patients with CHF caused by dilated cardiomyopathy (DCM) and ischemic cardiomyopathy (ICM) and 30 healthy controls (HC) were recruited in this study. Among the HF group, 34 and 30 patients were diagnosed as DCM and ICM, respectively. Written informed consent was obtained from all study participants. Inclusion criteria for the HF group were chronic stable HF diagnosed according to Framingham standards, New York Heart Association stage III-IV, and plasma prohormone of brain natriuretic protein (pro-BNP) content  $\geq 1,000$  ng/L. Exclusion criteria were defined as those patients with a history of myocardial infarction, percutaneous coronary intervention, coronary artery bypass grafting, coronary disease, iodine intolerance, poor renal function, or hemodynamically unstable patients.

The characteristics of the HF and control groups were shown in *Table 1*. The numbers of patients taking diuretics (64 patients), beta-adrenoceptor antagonists (62 patients), renin-angiotensin-aldosterone system (RAAS) inhibitors (60 patients), aspirin (30 patients), and statins (28 patients) were recorded. 15 patients had a history of arrhythmia (paroxysmal atrial fibrillation and/or nonsustained ventricular tachycardia), and 8 of them had implantable cardiac electrical defibrillators.

### *Plasma isolation and storage*

Whole venous blood sample was drawn from each participant. Samples were initially collected in ethylenediaminetetraacetic acid (EDTA)-containing tubes (Becton, Dickinson and Company) followed by a two-step centrifugal process (350 RCF (reactive centrifugal force) for 10 min and 20,000 RCF for 10 min (Beckman Coulter, USA) to isolate cell-free plasma samples within 12 hours. The obtained plasma samples were then restored in RNase-free tube at  $-80$  °C ready for future analysis. All of the collected plasma avoided freeze-thaw cycles.

**Table 1** Characteristics of heart failure patients (HF group) and healthy controls (HC group)

Characteristics	HF group (n=64)	HC group (n=30)	P value
Age (years)	58.8±12.9	59.2±12.1	0.57
Male/female (n/n)	39/25	18/12	0.94
Heart rate (bpm)	83.5±21.2	70.7±10.2	0.11
LVEF (%)	34.8±8.1	64.1±3.7	0.00
Log [BNP(ng/L)]	3.54±0.21	NA	NA
Current smoking, n (%)	10/64 (15.6%)	2/30 (0.07%)	0.00
Diabetes mellitus, n (%)	15/64 (23.4%)	0	0.00
Hypertension, n (%)	10/64 (15.6%)	0	0.00
SBP (mmHg)	104.6±11.6	109.8±10.5	0.58
DBP (mmHg)	74.4±13.8	80.8±12.6	0.41
ALT (U/L)	101.2±34.4	22.6±14.8	0.00
AST (U/L)	91.6±20.1	14.7±7.6	0.00
Cr (μmol/L)	121.9±21.6	74.9±16.6	0.02

Values are expressed as mean ± SD. LVEF, left ventricular ejection fraction as assessed by echocardiography; BNP, plasma brain natriuretic polypeptide (ng/L); NA, not available; SBP, systolic blood pressure; DBP, diastolic blood pressure; ALT, alanine aminotransferase (normal values: 0.0–45.0 U/L); AST, aspartate aminotransferase (normal values: 0.0–45.0 U/L); Cr, creatinine (normal values: 44.0–136.0 μmol/L).

### *miRNAs profiling screening and pathway enrichment analysis of differentially expressed genes (DEGs) in HF*

Expression profiling of miRNAs and mRNA by array or high throughput sequencing of human HF specimen were searched in Gene Expression Omnibus (GEO) database (<http://www.ncbi.nlm.nih.gov/geo/>). Two datasets of GSE53080 and GSE57338 were collected for further analysis because of larger sample size and relatively higher reliability of data.

The GSE53080 data derived from high throughput sequencing of myocardial and circulating miRNAs in human HF was downloaded and the “edgeR” (Empirical Analysis of Digital Gene Expression Data in R) was used to screen the miRNAs profiling between non-failing and failing heart samples. The significance analysis with |fold change (FC)| >2 and adj.P value <0.01 were chosen as the cut-off criteria to select miRNAs as the miRNA characteristic profiling of HF. The common variation of miRNAs in the myocardial and plasma samples of HF caused by DCM and ICM were collected for next step verification.

The GSE57338 data identified the myocardial gene expression signatures of HF by microarray. The GEO2R tool was used to find the DEGs between the non-failing and failing heart samples caused by DCM and ICM,

respectively. The DEGs were then uploaded to the Database for Annotation, Visualization and Integrated Discovery (DAVID) (<http://david.abcc.ncifcrf.gov/>), an online program providing a comprehensive set of functional annotation tools for investigators to understand biological meaning behind large list of genes, to perform KEGG pathway enrichment analysis. Those common terms including DEGs in the myocardial of HF caused by DCM and ICM were selected as the key biological process and pathways. P<0.05 was set as the cut-off criterion.

### *Plasma miRNAs extraction*

Total miRNAs were extracted using the mirVana PARIS Kit (Ambion, Austin, TX, USA) for each 200 μL plasma sample following the manufacturer’s instructions. The acquired total miRNAs were lysed into 100 μL RNase-free water and kept at –80 °C until analysis. The ultraviolet spectrophotometer was applied to evaluate the concentration and purity of total miRNAs samples. If the concentration of total miRNAs was less than 10 ng/μL, it was not included in data analysis. During the process, additional 5 μL of synthetic *C.elegans* miR-39 (cel-miR-39) (5 nM/L, RiboBio, Guangzhou, China) was added to each

sample after denaturing solution (Ambion, Austin, TX, USA) for sample-to-sample normalization.

#### *qRT-PCR for miR-216a detection*

miRNAs were amplified using Bulge-Loop<sup>TM</sup> miRNA quantitative reverse transcription polymerase chain reaction (qRT-PCR) Primer Set (RiboBio, Guangzhou, China) with specific primers of RT and PCR. According to previous study, RT and PCR procedures were performed on 7900HT real-time PCR system (Applied Biosystems, Foster City, CA, USA) in the condition of 42 °C for 60 min followed by 70 °C for 10 min (for RT) and 95 °C for 20 sec, followed by 40 cycles of 95 °C for 10 sec, 60 °C for 20 sec and then 70 °C for 10 sec (for PCR), respectively. SYBR Green (SYBR<sup>®</sup> Premix Ex Taq<sup>TM</sup> II, TaKaRa, Dalian, China) was used to calculate the amount of PCR products by the level of fluorescence and melting analysis was introduced to evaluate the specificity of PCR products. As our previously described, the expression levels of plasma miR-216a relative to exogenous reference miRNA (cel-miR-39) were quantified by the value of  $2^{-\Delta Ct}$  ( $\Delta Ct = Ct_{miR-216a} - Ct_{cel-miR-39}$ ) and then the relative FCs of plasma miR-216a between HF and HC groups were calculated by the value of  $2^{-\Delta\Delta Ct}$  ( $\Delta\Delta Ct =$  the average  $\Delta Ct$  of HF group - the average  $\Delta Ct$  of HC group) (5).

#### *Cell culture and treatment*

The HCF cell line was purchased from Cell Bank of Tongpai Biotechnology Co., Ltd. (Shanghai, China). Dulbecco's Modified Eagle's Medium (DMEM, Gibco Inc.) was formulated as the cell culture medium for HCF cells. In order to make the complete growth medium, the following components of 4.5 g/L glucose and fetal bovine serum were added in the base medium with the final concentration of 10%. Exponentially growing cultures were maintained in a humidified atmosphere of 5% carbon dioxide (CO<sub>2</sub>) at 37 °C.

#### *Transient transfections*

HCF cells were seeded in 6-well plates ( $6 \times 10^5$  cells/well). HCF cells were transfected with miR-216a mimic (100 nM) or miRNA mimic control (100 nM) using Lipofectamine<sup>TM</sup> 2000 reagent (Life Technologies, Carlsbad, CA, USA) according to the manufacturer's protocol, respectively. The miR-216a mimic and miRNA mimic control were purchased from Integrated Biotech

Solutions Co., Ltd (Shanghai, China).

#### *Cell proliferation assay*

The cell counting kit-8 (CCK-8) (Dojindo Molecular Technologies, Inc., Japan) method was used to analyze the cell growth of HCF cells according to the manufacturer's instructions. Six hours after the transfection of miR-216a mimic or miRNA mimic control in the HCF cells, the cells were then seeded with a density of  $5 \times 10^3$  cells/well in 96-well plates for total 24, 48, 72 hours at 37 °C with 5% CO<sub>2</sub>, respectively. The medium of each well was then substituted with 100  $\mu$ L of fresh medium containing 10% CCK-8, and the cultures were incubated at 37 °C for 2 hours. The absorbance value (A) was determined using Synergy<sup>TM</sup> 2 Multi-Mode Microplate Reader (BioTek Instruments, Inc., headquartered in Winooski, VT, USA) at 450 nm. Cell viability (%) = average absorbance of treated group/average absorbance of control group  $\times 100\%$ .

#### *Clonogenic assay*

HCF cells were transfected with miR-216a mimic or miRNA mimic control and then plated in 6-well plates at a density of 250 cells per well, incubated at 37 °C for two weeks, fixed, and stained with crystal violet. Colonies containing more than 50 cells were counted under a microscope from three independent replicates. Results are expressed as mean  $\pm$  SD.

#### *Dual-luciferase activity assay*

The 3'UTRs of human PTEN and SMAD7 cDNA containing the putative target site for the miR-216a (sequence shown in Supplementary data) were chemically synthesized and inserted at the XbaI site, immediately downstream of the luciferase gene in the pGL3-control vector (Promega, Madison, WI, USA) by Integrated Biotech Solutions Co., Ltd (Shanghai, China), respectively. Twenty-four hours before transfection, cells were plated at  $1.5 \times 10^5$  cells/well in 24-well plates. Two hundred ng of pGL3-PTEN-3'-UTR or pGL3-SMAD7-3'-UTR plus 80 ng pRL-TK (Promega) were transfected in combination with 50 nM of the miR-216a mimic or miRNA mimic control using Lipofectamine<sup>TM</sup> 2000 reagent (Life Technologies, Carlsbad, CA, USA) according to the manufacturer's protocol, respectively. Luciferase activity was measured

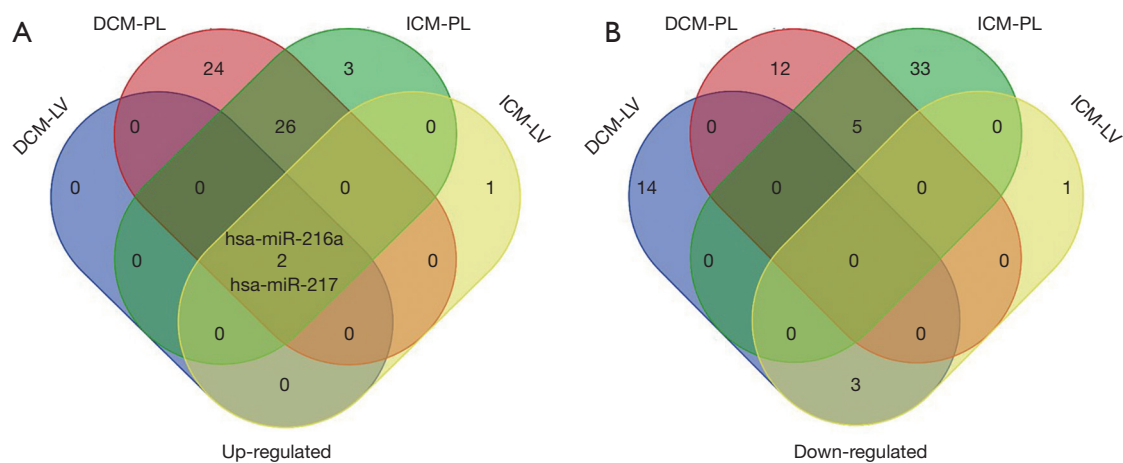


**Figure 1** Analysis of the common miRNAs alterations in both the myocardium tissues and the plasma of DCM-HF and ICM-HF. (A) MiR-216a and miR-217 were significantly up-regulated in common; (B) no miRNAs with obvious down-regulated expression level in common was found. DCM-HF, heart failure caused by dilated cardiomyopathy; ICM-HF, heart failure caused by ischemic cardiomyopathy.

24 hours after transfection using the Dual Luciferase Reporter Assay System (Promega). Firefly luciferase activity was normalized to renilla luciferase activity for each transfected well. Three independent experiments were performed in triplicate.

### Western blotting

HCF cells were seeded in 6-well plates ( $6 \times 10^5$  cells/well), cultured for 72 hours followed by transfection with miR-216a mimic or miRNA mimic control. Total protein was extracted from the cells and separated on 10% sodium dodecyl sulfate-polyacrylamide gels. Western blot was carried out as our previously described (5). Antibodies for the fibrogenesis indicator proteins of collagen I  $\alpha 2$  (catalog: ab96723) and fibronectin (catalog: ab32419); antibodies for the miR-216a targets of Smad7 (catalog: ab90086) and PTEN (catalog: ab32199); antibodies for effector proteins of PI3K-Akt and TGF- $\beta 1$ -Smads signal pathways including phosphorylated-pan-Akt (catalog: ab38449)/phosphorylated-mTOR (catalog: ab1093) and TGF- $\beta$ RI (catalog: ab31013)/phosphorylated-Smad2 (catalog: ab53100) and antibodies for reference protein of GAPDH (glyceraldehyde-3-phosphate dehydrogenase) (catalog: ab8245) were all purchased from Abcam. The expression level of each protein was normalized to that of GAPDH and FCs were calculated.

### Statistical analysis

All experiments were carried out more than 3 times. Numerical results are presented as mean  $\pm$  SD. Student's *t*-test was used to analyze the difference between means using SPSS13.0 software (Chicago, IL). Significance was indicated as \* $P < 0.05$ , # $P < 0.05$ , \*\* $P < 0.01$ , ## $P < 0.01$  and \*\*\* $P < 0.001$ . \* and # represented different gene in the same figure.

## Results

### MiR-216a was closely related to HF

The miRNAs profiling screening of HF was based on the high throughput sequencing data from the dataset of GSE53080. The miRNAs signatures in the left-ventricular myocardium and the plasma of HF patients caused either by DCM or ICM were shown in *Tables S1, S2*, respectively. Analysis of the common miRNAs alterations in both the myocardium tissues and the plasma of HF patients caused either by DCM or ICM verified that the mature members of miR-216a and miR-217 derived from the miR-216a/217 cluster were significantly up-regulated (*Figure 1A*), especially the miR-216a, while no miRNAs with obvious down-regulated expression level in common was found (*Figure 1B*).

MiR-216a/217 cluster was on the chr2 and could be

detected in endothelial cells exposed to hypoxia via deep-sequencing (9). As the pathophysiological essence of CHF was long-term hypoxia of organs (10), the mature members of the miR-216a/217 cluster might be also involved in HF. Exactly, the qRT-PCR further confirmed that the miR-216a was significantly up-regulated in the plasma of the HF patients with the average fold increment of 4.727, compared with the HCs (*Figure 2*,  $***P<0.001$ ).

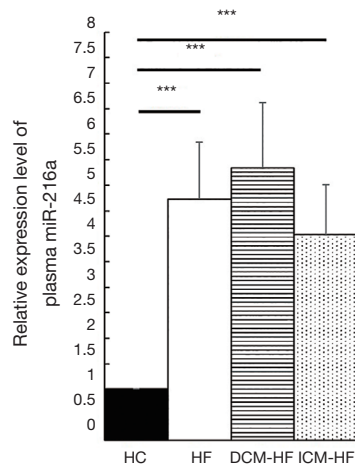


**Figure 2** MiR-216a was significantly up-regulated with the average fold increment of 4.727 in the plasma of the heart failure patients compared with the healthy controls. Moreover, it was consistently over-expressed in the plasma of DCM-HF and ICM-HF patients, with the average fold changes of 5.336 and 4.036, respectively.  $***P<0.001$ .

Moreover, the plasma miR-216a was consistently over-expressed in HF patients caused either by DCM or ICM, with the average FCs of 5.336 and 4.036, respectively (*Figure 2*,  $***P<0.001$ ). Those suggested that miR-216a was closely related to HF.

### *MiR-216a promoted proliferation and enhanced the fibrogenesis in HCF cells*

Since the fibrosis served as the pathological matrix of the HF, the potential role of miR-216a on HCF cells was studied. In HCF cells, the CCK-8 cell proliferation assay revealed that cells transfected with miR-216a mimic exhibited a significant increase of cell viability, compared with those transfected with miRNA mimic control. The P value of 24 hours, 48 hours and 72 hours are 0.037, 0.005, 0.002, respectively (*Figure 3A*). Clonogenic assay also confirmed that miR-216a could accelerate the proliferation of HCF cells. Those transfected with miR-216a mimic showed strong enhancement of clonogenic ability, compared with those transfected with miRNA mimic control (*Figure 3B*,  $P=0.003$ ). Meanwhile, the indicator proteins of the fibrogenesis of collagen I  $\alpha$  2 and fibronectin were significantly up-regulated in those HCF cells transfected with miR-216a mimic, compared with those transfected with miRNA mimic control (*Figure 3C*,  $**P=0.007$ ,  $##P=0.005$ ). The above indicated that miR-216a could promote the proliferation and enhance the fibrogenesis in HCF cells, which might induce the fibrosis in HF.

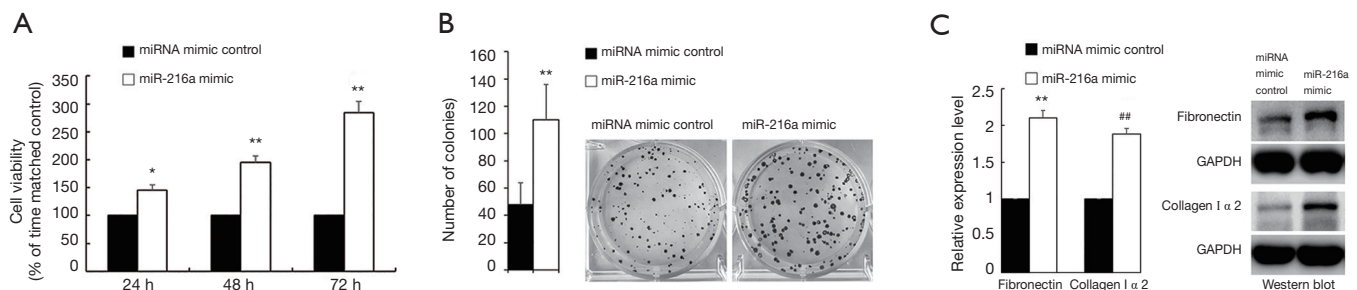


**Figure 3** MiR-216a promoted proliferation and enhanced the fibrogenesis in HCF cells. (A) The CCK-8 cell proliferation assay revealed that cells transfected with miR-216a mimic exhibited a significant increase of cell viability, compared with those transfected with miRNA mimic control; (B) clonogenic assay confirmed that miR-216a could accelerate the proliferation of HCF cells; (C) the indicator proteins of the fibrogenesis of collagen I  $\alpha$  2 and fibronectin were significantly up-regulated in those HCF cells transfected with miR-216a mimic, compared with those transfected with miRNA mimic control.  $*P<0.05$ ,  $**P<0.01$ ,  $##P<0.01$ , \* and # represented different gene in the same figure.



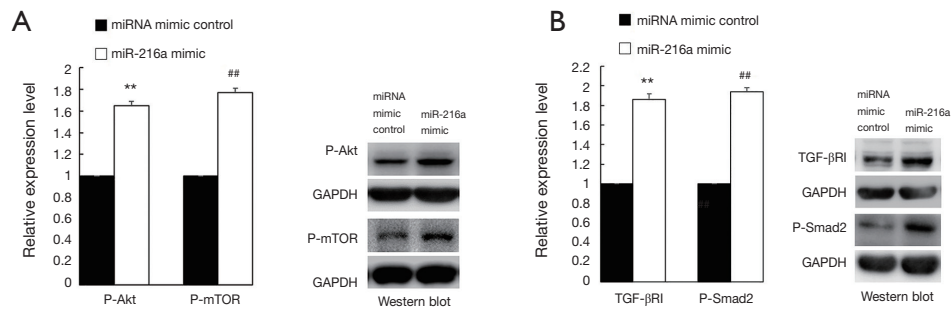


**Figure 5** Akt/mTOR and TGF-βRI/Smad2 were activated by miR-216a in HCF cells. (A,B) In HCF cells, at 72 hrs after transfection, western blot revealed that the expression of P-Akt, P-mTOR, TGF-βRI and P-Smad2 were all significantly up-regulated in cells transfected with miR-216a mimic compared with those transfected with miRNA mimic control, respectively. \*\* $P < 0.01$ , ## $P < 0.01$ , \* and # represented different gene in the same figure.

Since both PTEN and SMAD7 were the direct targets of miR-216a as mentioned above, we hypothesized that the activation of Akt/mTOR and TGF-βRI/Smad2 in HCF cells could be induced by miR-216a, which constituted the intrinsic molecular mechanism of proliferation promoting and fibrogenesis enhancement by miR-216a in HCF cells.

To verify this, HCF cells were transfected with miR-216a mimic and miRNA mimic control to detect changes in the expression levels of the effector proteins of P-Akt/P-mTOR and TGF-βRI/P-Smad2, which belonged to PI3K-Akt and TGF-β1-Smads signal pathways, respectively. In HCF cells, at 72 hours after transfection, western blot revealed that the expression of P-Akt, P-mTOR, TGF-βRI and P-Smad2 were all significantly up-regulated in cells transfected with miR-216a mimic compared with those transfected with miRNA mimic control, respectively (Figure 5A, \*\* $P = 0.006$ , ## $P = 0.005$ ; Figure 5B, \*\* $P = 0.004$ , ## $P = 0.003$ ).

Taken all together, we found that miR-216a accelerates proliferation and fibrogenesis in HCF cells via targeting PTEN and SMAD7 leading to the activation of Akt/mTOR and TGF-βRI/Smad2.

## Discussion

CHF is a progressive disease with relatively poor prognosis and lacks effective therapy. Myocardial fibrosis leading to ventricular remodeling is a common pathology of CHF, although there are many factors (1-3). Aberrant expressions of miRNAs act as biomarkers in the development and progression of CHF. MiRNAs are widely involved in the process of CHF, including interstitial fibrosis, myocardial hypertrophy, myocardial ischemia, and cellular

proliferation and apoptosis (7). In this study, analysis of the common miRNAs alterations was performed on both the myocardium tissues and the plasma of HF patients and we identified 2 up-regulated miRNAs. The expression of miR-216a was then confirmed markedly increased in the plasma of HF patients. Previous studies have described the role of miR-216a in HF. Menghini *et al.* found that miR-216a had a certain effect on the pathogenesis of cardiovascular disorders and atherosclerosis by controlling ox-LDL induced autophagy in HUVECs (13). Barsanti showed that miR-216a-5p was involved in focal adhesion/integrin pathway and in actin cytoskeleton regulation (14). However, very little was known about miR-216a and its biological effects on myocardial fibrosis. In our study, miR-216a was explored in our study and over-expression of miR-216a significantly was founded to promote viability, proliferation and enhanced the fibrogenesis in HCF cells. Taken together, these results indicate that miR-216a acts as a pathogenetic miRNA exerting an important effect on CHF progression.

PTEN is localized in chromosome 10, a lipid phosphatase and dual specificity protein. The lipid phosphatase activity is critical for its suppressor function, which negatively regulate PI3K-Akt signaling pathway by dephosphorylation and thereby modulate cell cycle progression and cell survival (11). Deleting PTEN was recently revealed to have a positive effect on cell proliferation and neuronal growth during development (15). Zhou *et al.* reported that downregulating expression of PTEN and Smad7 activate profibrotic signaling pathways (16). SMAD7 has been identified as a member of SMAD family, binding SMURF2 and targeting the TGF-β1 receptors especially the TGF-

$\beta$ RI for degradation through ubiquitination (12).

It has been reported that degradation of Smad7 may serve as a key mechanism for AF-induced atrial fibrosis (17). Lei *et al.* found that increasing Smad7 expression results in reduced collagen production and  $\alpha$ -smooth muscle actin expression in the activated HSCs (18). Those indicated that both PTEN and SMAD7 were closely related with fibrosis. In this study, we found that PTEN and SMAD7 were the direct targets of miR-216a in CHF. MiR-216a down-regulated PTEN and SMAD7 expression post-transcriptionally through binding to the 3'UTR of PTEN and SMAD7 which was verified by the luciferase reporter assay and western blot analysis.

In addition, our data also suggested that miR-216a/PTEN axis regulated cell viability and cell proliferation by Akt/mTOR signaling pathways and miR-216a/SMAD7 axis regulated fibrogenesis by involving in the TGF- $\beta$ RI/Smad2 signaling pathways. It has been well known that Akt/mTOR signaling pathway has an effect on cell cycle and proliferation and TGF- $\beta$ RI/Smad2 signaling pathway plays a key role in cell fibrogenesis (19,20). Since PTEN is a negative regulator of Akt/mTOR signaling pathways and SMAD7 antagonize of TGF- $\beta$ 1-Smads signaling (11,12), our study further showed that miR-216a mimic heighten the activation of the above two signaling pathways in the HCF cells. Therefore, we considered that miR-216a activated the above two signaling pathways by direct degradation of PTEN and SMAD7 in HCF cells. However, the specific mechanisms underlying the activation remains poorly understood and further investigations are needed.

## Conclusions

In conclusion, the results of our study showed that miR-216a was up-regulated in both tissues and the plasma of HF patients. It might be a potential marker for early HF screening. Importantly, miR-216a might act as a promoter of cardiac fibrosis through inducing proliferation and enhancing fibrogenesis in the HCF cells, at least via direct targeting the PTEN and SMAD7, leading to the activation of Akt/mTOR and TGF- $\beta$ RI/Smad2 signals in the HCF cells. These data might provide a promising approach for the treatment of CHF in the future.

## Acknowledgments

**Funding:** This study was funded by the National Natural Science Foundation of China (grant No. 81571873), Jiangsu

Province “333” project (grant No. BRA2017547) and Jiangsu Province Key Medical Talents project (grant No. ZDRCA2016016).

## Footnote

**Conflicts of Interest:** The authors have no conflicts of interest to declare.

**Ethical Statement:** The authors are accountable for all aspects of the work in ensuring that questions related to the accuracy or integrity of any part of the work are appropriately investigated and resolved. The animals in this study were obtained from the Animal Experimental Center of Nanjing Medical University. All animals handling and procedures were approved by the Animal Ethics Committee of Nanjing Medical University.

## References

1. Segura AM, Frazier OH, Buja LM, et al. Fibrosis and heart failure. *Heart Fail Rev* 2014;19:173-85.
2. Passino C, Barison A, Vergaro G, et al. Markers of fibrosis, inflammation, and remodeling pathways in heart failure. *Clin Chim Acta* 2015;443:29-38.
3. Schirone L, Forte M, Palmerio S, et al. A Review of the Molecular Mechanisms Underlying the Development and Progression of Cardiac Remodeling. *Oxid Med Cell Longev* 2017;2017:3920195.
4. Cheng R, Dang R, Zhou Y, et al. MicroRNA-98 inhibits TGF- $\beta$ 1-induced differentiation and collagen production of cardiac fibroblasts by targeting TGFBR1. *Human Cell* 2017;30:192-200.
5. Zou M, Wang F, Gao R, et al. Autophagy inhibition of hsa-miR-19a-3p/19b-3p by targeting TGF- $\beta$  R II during TGF- $\beta$ 1-induced fibrogenesis in human cardiac fibroblasts. *Sci Rep* 2016;6:24747.
6. Beaumont J, López B, Hermida N, et al. microRNA-122 down-regulation may play a role in severe myocardial fibrosis in human aortic stenosis through TGF-1 up-regulation. *Clin Sci (Lond)* 2014;126:497-506.
7. Chen C, Ponnusamy M, Liu C, et al. MicroRNA as a Therapeutic Target in Cardiac Remodeling. *Biomed Res Int* 2017;2017:1278436.
8. Travers JG, Kamal FA, Robbins J, et al. Cardiac Fibrosis: The Fibroblast Awakens. *Circ Res* 2016;118:1021-40.
9. Voellenkle C, Rooij JV, Guffanti A, et al. Deep-sequencing of endothelial cells exposed to hypoxia reveals

- the complexity of known and novel microRNAs. *RNA* 2012;18:472-84.
10. Zhao DS, Chen Y, Jiang H, et al. Serum miR-210 and miR-30a expressions tend to revert to fetal levels in Chinese adult patients with chronic heart failure. *Cardiovasc Pathol* 2013;22:444-50.
  11. Costa HA, Leitner MG, Sos ML, et al. Discovery and functional characterization of a neomorphic PTEN mutation. *Proc Natl Acad Sci U S A* 2015;112:13976-81.
  12. Kavsak P, Rasmussen RK, Causing CG, et al. Smad7 binds to Smurf2 to form an E3 ubiquitin ligase that targets the TGF beta receptor for degradation. *Mol Cell* 2000;6:1365-75.
  13. Menghini R, Casagrande V, Marino A, et al. MiR-216a: a link between endothelial dysfunction and autophagy. *Cell Death Dis* 2014;5:e1029.
  14. Barsanti C, Trivella MG, D'Aurizio R, et al. Differential regulation of microRNAs in end-stage failing hearts is associated with left ventricular assist device unloading. *Biomed Res Int* 2015;2015:592512.
  15. Knafo S, Esteban JA. PTEN: Local and Global Modulation of Neuronal Function in Health and Disease. *Trends Neurosci* 2017;40:83-91.
  16. Zhou X, Zang X, Ponnusamy M, et al. Enhancer of Zeste Homolog 2 Inhibition Attenuates Renal Fibrosis by Maintaining Smad7 and Phosphatase and Tensin Homolog Expression. *J Am Soc Nephrol* 2016;27:2092-108.
  17. He X, Gao X, Peng L, et al. Atrial fibrillation induces myocardial fibrosis through angiotensin II type 1 receptor-specific Arkadia-mediated downregulation of Smad7. *Circ Res* 2011;108:164-75.
  18. Lei XF, Fu W, Kim-Kaneyama JR, et al. Hic-5 deficiency attenuates the activation of hepatic stellate cells and liver fibrosis through upregulation of Smad7 in mice. *J Hepatol* 2016;64:110-7.
  19. Yang W, Wu Z, Yang K, et al. BMI1 promotes cardiac fibrosis in ischemia-induced heart failure via the PTEN-PI3K/Akt-mTOR signaling pathway. *Am J Physiol Heart Circ Physiol* 2019;316:H61-9.
  20. Okuno K, Naito Y, Yasumura S, et al. Influence of dietary iron intake restriction on the development of hypertension in weanling prehypertensive rats. *Heart Vessels* 2018;33:820-5.

**Cite this article as:** Tao J, Wang J, Li C, Wang W, Yu H, Liu J, Kong X, Chen Y. MiR-216a accelerates proliferation and fibrogenesis via targeting PTEN and SMAD7 in human cardiac fibroblasts. *Cardiovasc Diagn Ther* 2019;9(6):535-544. doi: 10.21037/cdt.2019.11.06

The sequence of 3'UTR of human PTEN cDNA containing the putative target site for hsa-miR-216a, sequence in bold stands for the putative target site:

TAACGACTTCTCCATCTCCTGTGTAATCAAGGCCAGTGCTAAAATTCAGATGCTGTTAGTACCTACATCAGTCAA  
CAACTTACACTTATTTTACTAGTTTTCAATCATAATACCTGCTGTGGATGCTTCATGTGCTGCCTGCAAGCTTCT-  
TTTTTCTCATTAATAATAAAATATTTTGTAAATGCTGCACAGAAATTTTCAATTT**GAGATT**CTACAGTAAGCGTTTT  
TTTTCTTTGAAGATTTATGATGCACTTATTCATAGCTGTGAGCCGTTCCACCCTTTTGACCTTACACATTCTA-  
TTACAATGAATTTTGCAGTTTTGCACATTTTTTAAATGTCATTAAGTGTAGGGAATTTTACTTGAATACTGAATA  
CATATAATGTTTATATTAATAAGGACATTTGTGTTAAAAAGGAAATTAGAGTTGCAGTAAACTTTCAATGCTGCACA.

The sequence of 3'UTR of human SMAD7 cDNA containing the putative target site for hsa-miR-216a, sequence in bold stands for the putative target site:

ATACACTCGTATGATACTTCGACACTGTTCTTAGCTCAATGAGCATGTTTAGACTTTAACATAAGCTATTT  
TTCTAACTACAAAGGTTTAAATGAAACAAGAGAAGCATTCTCATTGGAAATTTAGCATTGTAGTGCTTTGA  
GAGAGAAAGGACTCCTGAAAAAAAACCT**GAGATT**TATTAAGAAAAAAATGTATTTTATGTTATATATAAATA  
TATTATTACTTGTAAATATAAAGACGTTTATAAGCATCATTATTTATGTATTGTGCAATGTGTATAAACAAG

**Table S1** miRNAs profiling of different expression levels in DCM-LV and ICM-LV, compared with NF-LV, respectively (data derived from GSE53080)

miRNAs	logFC	P value
DCM-LV (n=21) vs. NF-LV (n=8)		
hsa-miR-216a	5.34922568	1.15E-06
hsa-miR-217	4.57071115	1.39E-07
hsa-miR-520f	-2.0088055	1.32E-05
hsa-miR-520h	-2.048149	2.36E-05
hsa-miR-135b	-2.1073234	0.000117
hsa-miR-518b	-2.1860896	9.23E-09
hsa-miR-122	-2.2166994	0.000396
hsa-miR-520b-3p	-2.2207942	5.09E-07
hsa-miR-1283-5p(2)	-2.221652	7.61E-06
hsa-miR-520c	-2.2242195	6.40E-07
hsa-miR-518a-3p(2)	-2.3107055	8.67E-05
hsa-miR-512-3p(2)	-2.347669	4.72E-08
hsa-miR-518f	-2.3610083	1.48E-05
hsa-miR-518e-3p	-2.5972399	5.45E-07
hsa-miR-519d	-2.6338239	7.78E-10
hsa-miR-519c	-2.6617672	8.69E-08
hsa-miR-515-5p(2)	-2.6919151	3.13E-09
hsa-miR-520g	-2.7530425	3.39E-10
hsa-miR-509-3p(3)	-3.0228901	6.53E-05
ICM-LV (n=13) vs. NF-LV (n=8)		
hsa-miR-216a	6.8782266	7.05E-08
hsa-miR-217	6.2596708	7.33E-09
hsa-miR-217*	5.5906776	4.65E-05
hsa-miR-520f	-2.240264	4.81E-06
hsa-miR-10a*	-2.277497	1.36E-10
hsa-miR-520g	-2.373177	5.88E-06
hsa-miR-135b	-2.655824	1.46E-06

NF-LV, nonfailing left-ventricular myocardium; DCM-LV, failing DCM left-ventricular myocardium; ICM-LV, failing ICM left-ventricular myocardium; DCM, dilated cardiomyopathy; ICM, ischemic cardiomyopathy; FC, fold changes.

**Table S2** miRNAs profiling of different expression levels in DCM-PL and ICM-PL, compared with HC-PL, respectively (data derived from GSE53080)

miRNAs	logFC	P value
DCM-PL (n=8) vs. HC-PL (n=13)		
hsa-miR-208b	7.9921809	2.51E-17
hsa-miR-216a	7.4441689	2.17E-14
hsa-miR-208a	6.7829824	8.97E-14
hsa-miR-499	5.2036956	7.08E-15
hsa-miR-513c-5p	5.1231472	1.76E-06
hsa-miR-1(2)	4.8979672	1.17E-11
hsa-miR-944	4.8883575	1.60E-05
hsa-miR-499*	4.6793667	3.47E-06
hsa-miR-455-3p	4.6284301	7.99E-07
hsa-miR-509-3-5p	4.4853413	0.00104494
hsa-miR-206	4.4677125	1.49E-06
hsa-miR-125b-1*	4.3978527	1.07E-07
hsa-miR-95	4.2905823	6.66E-10
hsa-miR-133b	4.2852317	1.10E-07
hsa-miR-218-1*	4.2625669	0.00019229
hsa-miR-513a-5p(2)	4.1486541	4.16E-05
hsa-miR-3614-5p	4.045718	0.00011409
hsa-miR-488	4.0023486	4.09E-06
hsa-miR-214-3p	4.0011706	3.20E-10
hsa-miR-217	3.9382187	0.0001021
hsa-miR-195	3.8748363	3.12E-16
hsa-miR-133a(2)	3.737871	4.56E-07
hsa-miR-508	3.6428773	0.00023033
hsa-miR-3158*	3.6322142	0.00015716
hsa-miR-135b	3.4945447	0.00100959
hsa-miR-183*	3.4450495	1.94E-07
hsa-miR-514a(3)	3.3353377	6.89E-05
hsa-miR-31-5p	3.1539515	0.00038397
hsa-miR-16(2)	3.1523255	1.30E-12
hsa-miR-183	3.1413921	1.00E-05
hsa-miR-2115*	3.1344451	0.00063224
hsa-miR-96	2.9194241	1.78E-06
hsa-miR-3158	2.9155771	8.29E-07
hsa-miR-378	2.8862125	1.62E-07
hsa-miR-218(2)	2.6605498	0.00075893
hsa-miR-1908	2.5961252	0.0006315
hsa-miR-193b*	2.5884606	4.29E-05
hsa-miR-1180	2.5813098	4.24E-06
hsa-miR-18b*	2.5463065	0.00023238
hsa-miR-451-DICER1	2.4987946	2.72E-05
hsa-miR-3909	2.4519085	0.00084447
hsa-miR-424	2.3911302	2.24E-07
hsa-miR-378*	2.3750965	7.21E-05
hsa-miR-452*	2.3583024	4.39E-05
hsa-miR-148a	2.3309839	1.19E-06
hsa-miR-125b-2*	2.3038011	0.0002102
hsa-miR-193a-5p	2.2781728	9.42E-06
hsa-miR-100	2.1553314	0.00018549
hsa-miR-486	2.117182	0.00038519
hsa-miR-497	2.1134329	0.00048131
hsa-miR-193b	2.1041541	0.00090767
hsa-miR-3613	2.0282438	0.00038332
hsa-miR-654	-2.030205	0.00054335
hsa-miR-181d	-2.048155	1.54E-05
hsa-miR-380-3p	-2.153415	0.00110199
hsa-miR-369	-2.157492	0.00075554
hsa-miR-299-3p	-2.179875	0.0007853
hsa-miR-376b	-2.23972	0.00076698
hsa-miR-323b	-2.44516	8.34E-05
hsa-miR-409-5p	-2.560739	0.00053453
hsa-miR-411*	-2.606823	4.54E-05
hsa-miR-379*	-2.670715	0.00034308
hsa-miR-433	-2.791696	0.00029166
hsa-miR-127-3p	-2.818025	3.33E-06
hsa-miR-1249	-2.833118	9.80E-06
hsa-miR-382-5p	-2.902079	7.99E-05
hsa-miR-496	-3.050867	0.00013244
hsa-miR-543*	-3.123533	0.00098752
hsa-miR-758	-4.377876	5.06E-07
ICM-PL (n=17) vs. HC-PL (n=13)		
hsa-miR-216a	7.110835	1.22E-10
hsa-miR-208b	6.421233	2.73E-16
hsa-miR-208a	5.553521	3.24E-15
hsa-miR-499	4.356927	1.25E-10
hsa-miR-125b-1*	4.328145	5.05E-10
hsa-miR-133a(2)	4.265091	2.49E-06
hsa-miR-206	4.08374	2.47E-06
hsa-miR-214-3p	3.939473	4.41E-09
hsa-miR-217	3.845286	2.47E-05
hsa-miR-133b	3.661274	8.77E-06
hsa-miR-95	3.58138	1.69E-09
hsa-miR-513c-5p	3.547207	0.000240019
hsa-miR-1(2)	3.534353	5.20E-09
hsa-miR-99a*	3.438075	0.000207685
hsa-miR-195	3.435051	5.05E-16
hsa-miR-455-3p	3.34015	1.76E-05
hsa-miR-2115*	3.144821	0.000492927
hsa-miR-511-3p(2)	3.00785	0.000116896
hsa-miR-499*	2.938392	0.000818854
hsa-miR-16(2)	2.889578	2.60E-10
hsa-miR-488	2.884034	0.000617331
hsa-miR-218(2)	2.843637	0.001242513
hsa-miR-183*	2.599276	5.31E-05
hsa-miR-96	2.549596	3.04E-07
hsa-miR-451-DICER1	2.504176	7.31E-05
hsa-miR-18b*	2.428639	0.000173208
hsa-miR-3158	2.361108	2.13E-05
hsa-miR-424	2.352185	7.53E-09
hsa-miR-3909	2.246346	0.000714904
hsa-miR-125b-2*	2.184985	3.00E-05
hsa-miR-550-5p(2)	2.159456	2.55E-07
hsa-miR-654	-2.0018	3.01E-05
hsa-miR-379	-2.00325	2.24E-05
hsa-miR-412-5p	-2.05761	0.001002524
hsa-miR-382-5p	-2.0836	6.14E-05
hsa-miR-1307*	-2.0912	1.06E-07
hsa-miR-9(3)	-2.09869	1.80E-05
hsa-miR-21*	-2.11327	2.73E-07
hsa-miR-589	-2.12	5.76E-07
hsa-miR-1197	-2.13858	0.002144951
hsa-miR-33a*	-2.13927	0.000117887
hsa-miR-190a	-2.15388	2.42E-05
hsa-miR-181c	-2.18687	1.02E-09
hsa-miR-584	-2.18854	5.19E-08
hsa-miR-1250	-2.19158	6.37E-05
hsa-miR-1296	-2.21224	6.74E-06
hsa-miR-671*	-2.23617	4.49E-08
hsa-miR-374a*	-2.24361	6.49E-08
hsa-miR-146a*	-2.3096	0.000138853
hsa-miR-127-3p	-2.31099	2.84E-07
hsa-miR-331	-2.35872	1.08E-06
hsa-miR-1307	-2.36248	1.35E-08
hsa-miR-370	-2.43062	4.08E-09
hsa-miR-199a-5p(2)	-2.52853	9.51E-06
hsa-miR-301a*	-2.53885	0.000984122
hsa-miR-551b	-2.56297	7.01E-07
hsa-miR-375	-2.66014	7.74E-05
hsa-miR-181a-1*	-2.66586	1.85E-10
hsa-miR-136-5p	-2.8357	1.54E-08
hsa-miR-744*	-2.90019	2.95E-06
hsa-miR-181c*	-2.97673	1.05E-10
hsa-miR-381*	-3.03179	0.001265672
hsa-miR-136-3p	-3.10578	3.01E-06
hsa-miR-215	-3.13301	3.15E-07
hsa-miR-1277-3p	-3.19982	1.96E-07
hsa-miR-758	-3.42355	3.55E-07
hsa-miR-497*	-3.5878	0.000999439
hsa-miR-708*	-3.9966	0.002131476
hsa-miR-1249	-4.80367	6.99E-14

HC-PL, healthy control-plasma; DCM-PL, heart failure-DCM-plasma; ICM-PL, heart failure-ICM-plasma; DCM, dilated cardiomyopathy; ICM, ischemic cardiomyopathy; FC, fold changes.

**Table S3** The common altered pathway between DCM and ICM caused HF (data derived from GSE57338)

Input DEGs number	P value	KEGG term in DCM caused HF
13	1.4842E-06	Pathways in cancer
8	8.2197E-06	Jak-STAT signaling pathway
11	1.1289E-05	PI3K-Akt signaling pathway
5	7.1712E-05	Pancreatic cancer
6	0.00021517	FoxO signaling pathway
6	0.00033487	Hepatitis B
5	0.00092376	Thyroid hormone signaling pathway
4	0.00117379	Prolactin signaling pathway
5	0.00169372	Measles
4	0.001776	EGFR tyrosine kinase inhibitor resistance
6	0.00183865	Viral carcinogenesis
6	0.00183865	Proteoglycans in cancer
5	0.00285424	Hippo signaling pathway
6	0.00307471	Ras signaling pathway
3	0.00427176	Amyotrophic lateral sclerosis (ALS)
3	0.00449834	Mineral absorption
3	0.00573972	Acute myeloid leukemia
3	0.00657342	Viral myocarditis
4	0.00667029	Toxoplasmosis
2	0.00989834	Renin-angiotensin system
4	0.01145147	Apoptosis
2	0.01498383	Thyroid cancer
3	0.01628119	Insulin secretion
3	0.01677582	Small cell lung cancer
2	0.01887367	Apoptosis-multiple species
3	0.03046691	Insulin resistance
2	0.03144613	Vasopressin-regulated water reabsorption
2	0.04214279	Endometrial cancer
3	0.0425873	AMPK signaling pathway
2	0.04645711	Pathogenic Escherichia coli infection
6	0.00023063	Apoptosis
4	0.00055111	Viral myocarditis
9	0.00070249	Pathways in cancer
4	0.00077383	Pancreatic cancer
5	0.00201178	Hepatitis B
5	0.00251683	Hippo signaling pathway
7	0.00469104	PI3K-Akt signaling pathway
3	0.0048141	Pathogenic Escherichia coli infection
4	0.00585568	Thyroid hormone signaling pathway
4	0.00602526	Toxoplasmosis
5	0.00809503	Proteoglycans in cancer
2	0.00935855	Renin-angiotensin system
3	0.00979833	Prolactin signaling pathway
3	0.01330766	EGFR tyrosine kinase inhibitor resistance
2	0.01417636	Thyroid cancer
3	0.01506833	Insulin secretion
4	0.01539955	Jak-STAT signaling pathway
3	0.01552804	Small cell lung cancer
2	0.01786465	Apoptosis-multiple species
3	0.02828083	Insulin resistance
2	0.02980168	Vasopressin-regulated water reabsorption
4	0.03490069	Viral carcinogenesis
2	0.03863969	Amyotrophic lateral sclerosis (ALS)
3	0.0396085	AMPK signaling pathway
2	0.03997442	Mineral absorption
2	0.03997442	Endometrial cancer
3	0.04684502	FoxO signaling pathway
2	0.04690245	Acute myeloid leukemia
4	0.04801018	Ras signaling pathway
3	0.04853571	Measles

DCM, dilated cardiomyopathy; ICM, ischemic cardiomyopathy; HF, heart failure; DEGs, differentially expressed genes.